PAPER • OPEN ACCESS

Enhancing and reducing the Rashba-splitting at surfaces by adsorbates: Na and Xe on Bi/Cu(111)

To cite this article: Hendrik Bentmann and Friedrich Reinert 2013 *New J. Phys.* **15** 115011

New Journal of Physics
The open access journal for physics

Enhancing and reducing the Rashba-splitting at surfaces by adsorbates: Na and Xe on Bi/Cu(111)

Hendrik Bentmann[1,2,3] **and Friedrich Reinert**[1,2]

[1] Experimentelle Physik VII, Universität Würzburg, Am Hubland, D-97074 Würzburg, Germany

[2] Karlsruhe Institute of Technology KIT, Gemeinschaftslabor für Nanoanalytik, D-76021 Karlsruhe, Germany

E-mail: hendrik.bentmann@physik.uni-wuerzburg.de

New Journal of Physics **15** (2013) 115011 (16pp)
Received 31 May 2013
Published 19 November 2013
Online at http://www.njp.org/
doi:10.1088/1367-2630/15/11/115011

Abstract. The surface alloy Bi/Cu(111) shows a paradigmatic free-electron-like surface state with a very large Rashba-type spin–orbit splitting. Using angle-resolved photoemission we investigate how adsorbates of different chemical nature influence the size of the spin splitting in this system. We find that the adsorption of small amounts of monovalent Na atoms leads to an enhancement of the spin splitting while an overlayer of the closed-shell rare gas Xe causes a reduction. The latter result is in contrast to the Au(111) surface for which an increased splitting size after Xe-adsorption was observed. We discuss these experimental findings in terms of the characteristic differences of the surface state wave functions and their spatial deformation in the presence of different types of adsorbates. Our results provide insight into the complex interplay of atomic and interface potential gradients governing the Rashba effect.

[3] Author to whom any correspondence should be addressed.

Contents

1. Introduction

The spin degeneracy of electronic states at surfaces can be lifted by spin–orbit coupling because of the broken spatial inversion symmetry connected with the existence of the surface [1]. This mechanism, commonly referred to as Rashba effect [2], results in a momentum dependent splitting of states with opposite spin and induces a characteristic spin structure in momentum space [1]. The Rashba effect has attracted considerable interest in the field of spintronics. It can be utilized for the manipulation of spin currents at semiconductor interfaces [3–5] and lies at the origin of the intrinsic spin Hall effect [6]. More recent proposals discuss Rashba-type spin splittings as a route for the realization of exotic phenomena, such as Majorana fermions [7–9], or as a way to enhance many-body effects, such as Kondo scattering [10] and superconducting pairing [11, 12]. In all of the above cases control over the strength of the Rashba effect, that is the size of spin splitting, and ways to manipulate it are of crucial relevance. However, the splitting size and its dependence on adjustable structural or chemical interface parameters are often hard to predict even for simple systems as they result from a complex interplay of intra-atomic spin–orbit coupling and details of the interfacial potential gradients [13–17]. In this work we aim to improve the understanding of this interplay by comparing the influence of simple, yet chemically different adsorbate species (monovalent Na and closed-shell Xe) on the spin splitting in the surface alloy Bi/Cu(111), representing a paradigmatic model system with large spin–orbit interaction.

The Rashba effect in a two-dimensional electron gas (2DEG) gives rise to an isotropic splitting of the spin-degenerate parabolic dispersion into two spin-polarized branches [1]:

$$E_{\pm}(\mathbf{k}) = E_B + \frac{\hbar^2}{2m^*}\mathbf{k}^2 \pm \alpha|\mathbf{k}|. \tag{1}$$

Here, m^* is the effective electron mass and $\mathbf{k} = (k_x, k_y)$, with $|\mathbf{k}| = k$, is the wave vector within the interface plane. The size of the spin–orbit splitting is described by the Rashba parameter α. Along an arbitrary k-direction the dispersion is described by two parabolas of opposite spin direction that are shifted from the zone center ($k = 0$) by the constant wave vector offset $k_0 = \alpha m^*/\hbar^2$. At a given wave vector k the energy splitting between the branches $E_{\pm}$ is given by $\Delta E = 2\alpha k$.

Rashba-type spin splittings are commonly observed for surface states on crystal surfaces that incorporate heavy elements (see e.g. [18–20]). They can be detected directly by angle-resolved photoelectron spectroscopy (ARPES) which provides immediate access to the momentum-resolved electronic structure of surface and thin film systems [21]. Different experiments showed that the Rashba effect at surfaces depends on the atomic composition [22–24] and on the structural properties of the system [25–27]. The influence of adsorbates on the Rashba-splitting of surface states has been studied previously for different material combinations. ARPES experiments for the systems Li/W(110) [28], Xe, Ar/Au(111) [29–31] and O/Gd(0001) [32] showed increased splitting sizes as a result of the adsorption, whereas no change was found for the case of Xe on Bi/Ag(111) [33]. The basic physical mechanism behind these modifications is usually identified as an adsorbate-induced change of the surface potential and concomitant deformations of the surface state wave function. However, in order to gain a more comprehensive picture additional systematic experiments are required. The contrasting results for Xe-adsorption on Au(111) and Bi/Ag(111) indicate that the influence of a particular adsorbate may vary depending on the substrate surface. Up to now, no experimental study focused systematically on the influence of different adsorbates on the Rashba-splitting of a particular substrate.

Recently, long-range ordered surface alloys such as Bi/Ag(111) and Bi/Cu(111) have attracted considerable interest as they show well-defined, free-electron-like surface states with very large Rashba-splittings [20, 25, 34, 35]. In this paper we present a detailed ARPES study of the Rashba-splitting in Bi/Cu(111) and its modification after adsorption of Na and Xe. We find that both adsorbates change the splitting size by approximately 10% with respect to the clean surface alloy. Interestingly, the effect of the two chemically different species turns out to be opposite: Na-adsorption enhances the splitting size whereas Xe-adsorption leads to a reduction. In order to rationalize our experimental findings we propose a simple model based on the surface state wave function and its deformation after the adsorption. We also discuss the results in the light of previous experiments on other adsorbate–substrate combinations.

2. Experimental details

All experiments and surface preparation procedures were carried out in ultrahigh vacuum with a base pressure below 2×10^{-10} mbar. We performed ARPES experiments using a hemispherical electron spectrometer (Scienta R4000) and a monochromatized He discharge lamp. For all measurements we used a photon energy of $h\nu = 21.22$ eV (He Iα). The energy and angular resolution were 7 meV and 0.3°, respectively. A clean and ordered Cu(111) substrate was prepared by Ar-sputtering and annealing of a polished single crystal. We judged the surface quality by the energy line width of the L-gap surface state and by low-energy electron diffraction (LEED). The Bi/Cu(111) surface alloy was obtained by evaporating 1/3 ML Bi from a commercial Knudsen cell on the heated substrate. We confirmed the formation of the $(\sqrt{3} \times \sqrt{3})R30°$-reconstruction by LEED measurements. Na was deposited at a reduced sample temperature of approximately 150 K using a commercial alkali dispenser. The deposition rate was estimated from x-ray photoemission (XPS). Xe was adsorbed slowly at a sample temperature of 65 K and a partial pressure of 2×10^{-8} mbar leading to a thickness of slightly above 1 ML. During the adsorption process we monitored the evolution of the Xe $5p_{1/2}$ valence level. At full coverage we observed a clear dispersion of this feature by ARPES indicating the formation of an ordered Xe layer.

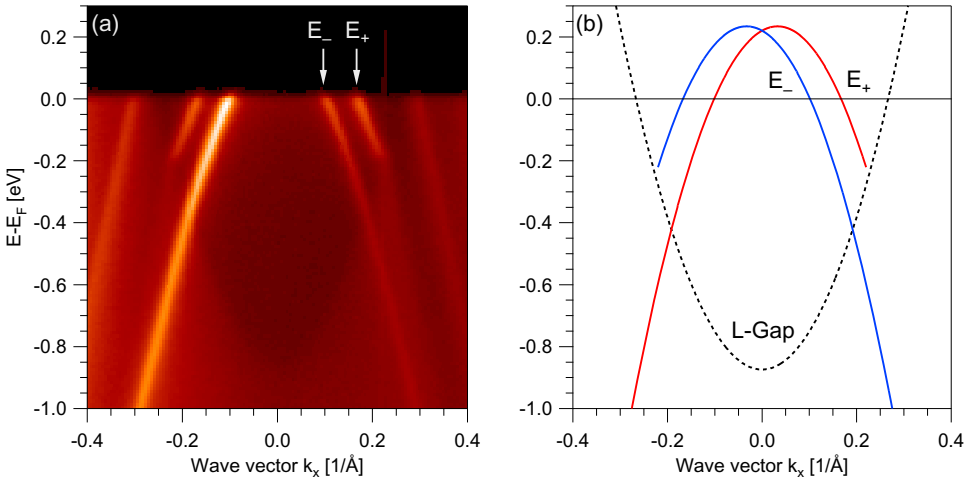

Figure 1. Electronic structure of the surface alloy Bi/Cu(111). A partially unoccupied, Rashba-split surface state $E_{\pm}$ within the projected bulk band gap of the substrate (L-gap) is revealed by the ARPES spectrum in (a). Another surface state band is visible at higher wave vectors. The parabolic L-gap is discerned in the data by its slightly lower background intensity compared to other parts of the spectrum. The sketch in (b) shows a schematic summary of the experimental data using the dispersion relation in equation (1).

3. Experimental results

3.1. Clean Bi/Cu(111)

The surface alloy Bi/Cu(111) has been studied previously by ARPES [25, 35, 36], scanning tunneling spectroscopy [35, 37], two-photon photoemission [36, 38], spin-resolved photoemission [39] as well as *ab initio* electronic structure calculations [25, 36, 38]. In the following we briefly introduce the relevant features in the electronic structure of this compound and discuss in slightly more detail the quantitative applicability of the Rashba-model in equation (1).

Figure 1(a) shows the electronic structure of Bi/Cu(111) as determined by ARPES. We find two inner bands which are identified as spin-split surface state branches $E_{\pm}$. This assignment has been confirmed previously by different experiments [25, 35] as well as density functional theory calculations [25]. The ARPES data shows a third band at larger wave vectors which is attributed to another surface state. According to previous theoretical results all observed bands are mainly derived from Bi states whereas the two inner spin-split branches are primarily of sp_z orbital character and the outer branch is of $p_x p_y$ character [25, 38]. In addition to the three band branches the spectrum in figure 1(a) allows one to discern the projected bulk band gap of the Cu(111) substrate (L-gap) that shows a reduced background intensity. Figure 1(b) gives a schematic summary of the relevant features in the electronic structure of Bi/Cu(111) as deduced from experiment.

As is evident from figure 1(a) the branch E_+ strongly hybridizes with bulk states when passing the edge of the projected L-gap which results in a strong blurring of its spectral weight. On the other hand the branch E_- shows a much weaker hybridization. The Rashba-model in

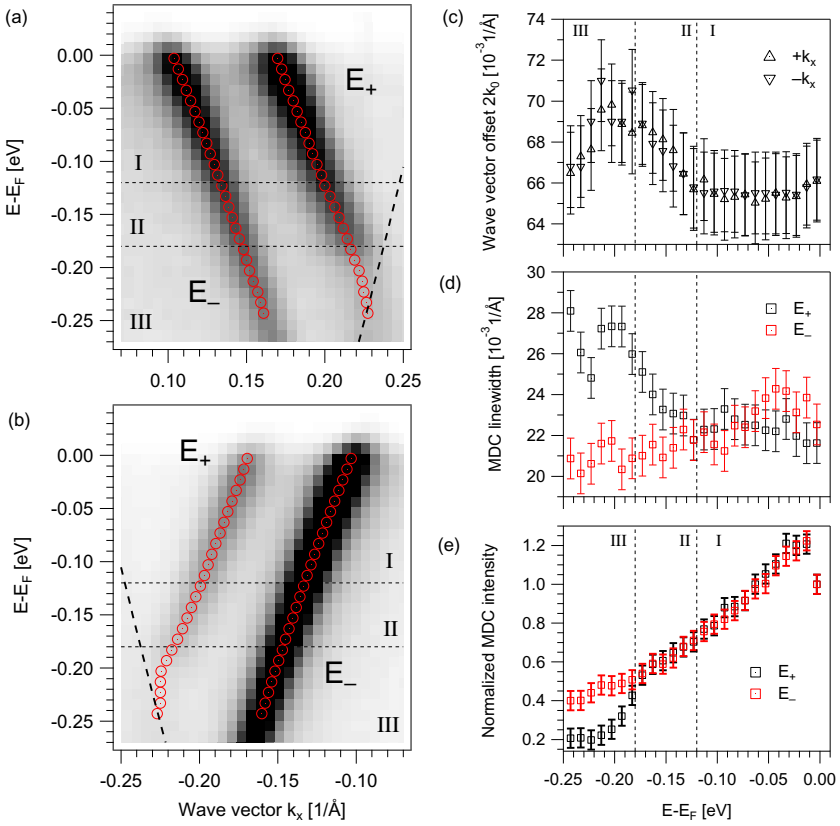

Figure 2. Quantitative analysis of the dispersion and the spectral behavior of the spin-split branches $E_{\pm}$ in Bi/Cu(111). Panels (a) and (b) show parts of the ARPES spectrum in figure 1(a) in more detail. The data points in (a) and (b) mark intensity maxima as determined by Lorentzian fits to the momentum distribution curves (MDC). The resulting wave vector offsets k_0 between the branches E_+ and E_-, the line widths and the peak intensities are plotted in (c)–(e), respectively.

equation (1) is thus only valid in a limited wave vector range. A quantitative analysis of the experimental dispersion is presented in figure 2. Detail plots from the APRES data in figure 1(a) are shown in figures 2(a) and (b). The data points denote intensity maxima that were obtained by fitting Lorentzian line shapes to MDC. The corresponding wave vector splitting k_0 between the branches E_+ and E_- as a function of energy is displayed in figure 2(c). As discussed above the Rashba-model in equation (1) predicts a constant, energy-independent wave vector offset. We find that this is indeed the case within the energy interval I. At higher binding energies the splitting first increases (interval II) and then tends to decrease again (interval III).

The deviations from the ideal dispersion in equation (1) can be traced back to the hybridization of the branch E_+ with bulk states close to the edge of L-gap. This is inferred from figures 2(d) and (e) where we plot the line widths and the peak intensities corresponding to the two bands. These spectral properties are expected to change as a result of the hybridization that induces a reduced lifetime and a more bulk-localized charge distribution of the states. Within energy interval I the spectral properties of the two branches show the same behavior. Going to interval II, however, we observe an increase in line width for E_+ that is not found for E_-. In

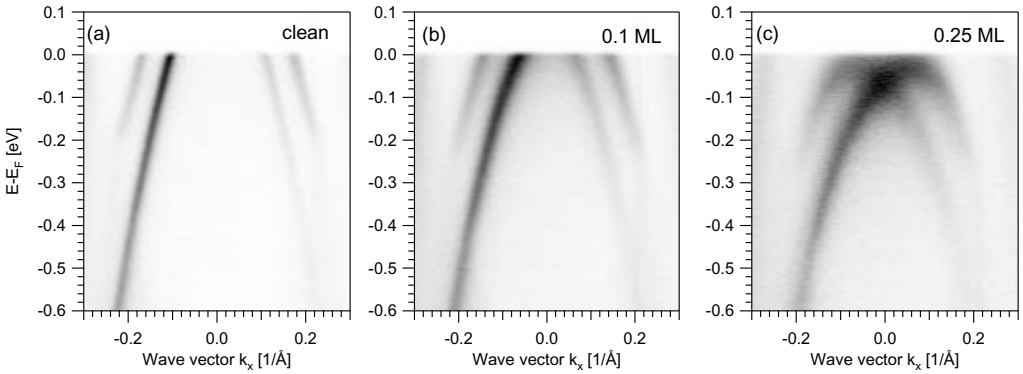

Figure 3. Effect of Na deposition on the electronic structure of Bi/Cu(111) as determined by ARPES at $T = 50$ K. Spectra for the clean surface alloy and after deposition of 0.1 and 0.25 ML are shown in (a)–(c), respectively.

interval III also the peak intensities start to deviate from each other and become reduced for E_+ as compared to E_-. Hence, the spectral properties show changes in their energy dependence at the same energies as the wave vector offset k_0, strongly suggesting hybridization with bulk states as a common origin. Summarizing our analysis we conclude that within interval I the branches $E_\pm$ behave as well-defined surface states, meaning they are decoupled from the three-dimensional bulk electronic structure. Here, also their spin-splitting precisely follows the predictions of the Rashba-model for a 2DEG.

Before proceeding we briefly comment on the observed hybridization effect at the L-gap edge. The surprising aspect here is the strong difference in hybridization with bulk states for the two branches E_+ and E_- that has also been observed for the related surface alloys Bi/Ag(111) [20] and Pb/Ag(111) [40]. As these two branches carry opposite spin, as shown experimentally in [34, 39], the hybridization appears to be spin-selective. The hybridization strength, however, is expected to be determined by the symmetry of the spatial part of the wave function, meaning the orbital part, and its match with the symmetry of the substrate states. In the present case, spin–orbit coupling is strong and thus will cause entanglement of orbital and spin wave function parts [41]. As a result the branches E_+ and E_- are not only of opposite spin but also of different orbital symmetry [38, 42]. We speculate that this spin–orbit-induced entanglement could be the origin for the selective hybridization.

3.2. Na-adsorption on Bi/Cu(111)

Previous studies on the surface alloys Bi/Cu(111) and Bi/Ag(111) showed that alkali adsorption increases the binding energy of the Rashba-split surface states, thereby allowing to manipulate the parameter E_B in equation (1) [25, 43]. This effect is illustrated in figure 3 where we present ARPES measurements of Bi/Cu(111) before and after deposition of Na. The spectra provide evidence for a coverage dependent shift of the band $E_\pm$. This shift to higher binding energy is attributed to charge transfer from the monovalent Na atoms to the states of the surface alloy. In the following we will focus on adsorption-induced modifications of the parameters k_0 and ΔE that quantify the size of the spin-splitting. To this end we compare ARPES data for clean Bi/Cu(111) and after deposition of 0.1 ML Na.

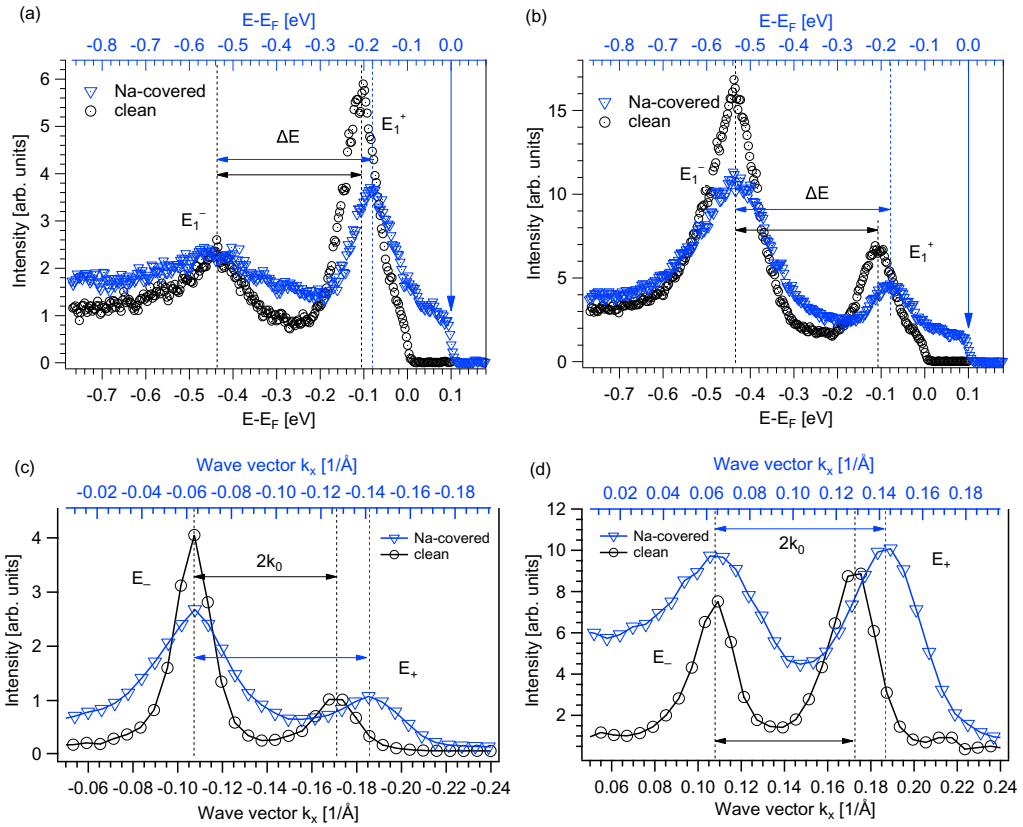

Figure 4. Energy distribution curves (EDC) at $k_x = 0.2\,\text{Å}^{-1}$ in (a) and $k_x = -0.2\,\text{Å}^{-1}$ in (b) and MDC at the Fermi energy E_F in (c) and (d) for Bi/Cu(111) before and after deposition of 0.1 ML Na. The spin-split branches E_+ and E_- show up as two peaks in every EDC and every MDC. For a better comparison of the energy separation ΔE (wave vector offset k_0) the energy axes (wave vector axes) for the clean (black) and the Na-covered (blue) surface alloy were shifted by 100 meV (0.044 Å^{-1}) with respect to each other.

Figure 4 shows EDC for the clean (black) and the Na-covered (blue) surface alloy at wave vectors of $k_x = \pm 0.2\,\text{Å}^{-1}$ in (a) and (b). All EDC show two peaks that are associated with the two branches E_+ and E_-. The energy separation of these peaks directly reflects the spin-splitting ΔE. Note that the energy axes of the EDC for the clean (lower axis) and the Na-covered (upper axis) surface alloy are shifted by 100 meV with respect to each other in figures 4(a) and (b). In doing so the peak positions of the branch E_- match each other and a change in the separation between E_+ and E_- is easier to recognize. As is evident from the EDC the energy splitting ΔE is larger for the Na-covered surface alloy providing direct evidence for an adsorption-induced enhancement of the Rashba-splitting. Apart from the increase in ΔE one can also discern a substantial increase in the line width of the peaks as a result of the adsorption. We attribute this broadening to disorder being introduced by the randomly distributed Na atoms.

To further examine the effect of Na-adsorption on the spin-splitting we consider MDC at the Fermi energy E_F in figures 4(c) and (d). The panels show the relevant parts of the MDC at negative and positive wave vectors in (c) and (d), respectively. In each spectrum we identify

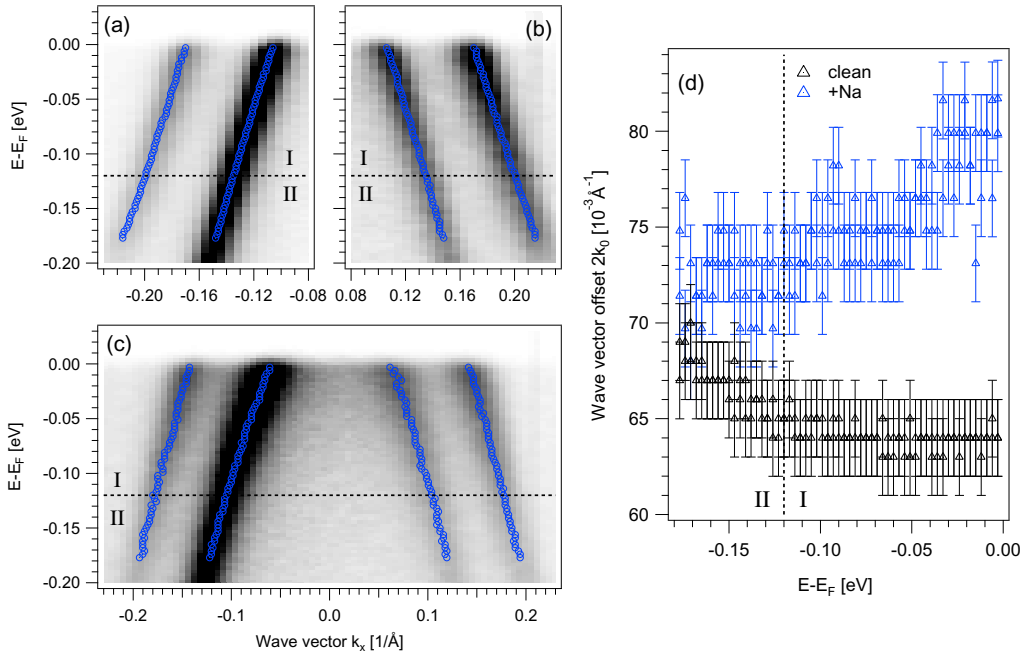

Figure 5. Quantitative analysis of the dispersion of the Rashba-split branches $E_{\pm}$ in Bi/Cu(111) before and after deposition of 0.1 ML Na. Panels (a) and (b) show parts of the spectrum in figure 3(a) for the clean surface alloy in more detail. A corresponding image section from figure 3(b) for the Na-covered surface alloy is displayed in (c). The data points in (a)–(c) denote intensity maxima. The corresponding wave vector offsets k_0 are plotted in (d).

two peaks that are related to the branches E_+ and E_-. The wave vector separation of these peaks corresponds to $2k_0$. Similar as for the EDC the axes of the MDC for the clean and the Na-covered surface alloy were shifted by 0.044 Å^{-1} with respect to each other so that the peak positions of the branch E_- coincide. Comparing the determined wave vector offsets one finds an increase in the splitting parameter k_0 as a result of the adsorption. Note that k_0 depends on the effective mass and thus does not provide direct information on the Rashba-splitting parameter α.

A full analysis of the dispersion of the state $E_{\pm}$ is presented in figure 5. Detail plots for clean and Na-covered Bi/Cu(111) are shown in panels (a)–(c). The data points in these graphs denote intensity maxima obtained from MDC. The resulting wave vector offsets k_0 are plotted as a function of energy in panel (d). The energy axes in figure 5 are divided into the two intervals I and II according to the discussion in section 3.2. The data shows that the splitting k_0 is increased within the full energy range that is considered here. One also finds that, within interval I, k_0 is not fully constant as observed for the clean surface alloy but rather shows a small reduction with increasing binding energy. This observation might result from a k-dependent effective mass m^* as consequence of the specific band structure. Despite these minor deviations from the Rashba-model we performed a least square fit of equation (1) to the data in figure 5 within interval I. Resulting from this we deduce a Rashba-parameter of $\alpha = 0.845(30)$ eV Å for clean Bi/Cu(111) and $\alpha = 0.93(3)$ eV Å after deposition of 0.1 ML Na.

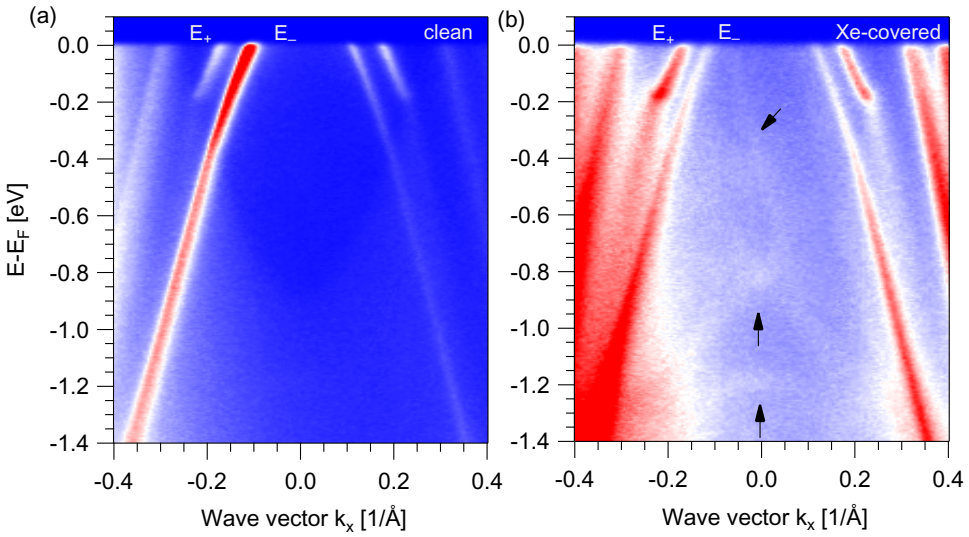

Figure 6. Influence of Xe-adsorption on the electronic structure of Bi/Cu(111) as determined by ARPES. Panels (a) and (b) show spectra for the clean surface and after adsorption of ∼1 ML Xe, respectively. In (b) faint shadow bands are observed and denoted by arrows. These bands are attributed to backfolded replicas of the surface state branches as a result of the superstructure of the Xe-overlayer. A false-color depiction of the data is used to improve the visibility of all spectral features.

Summarizing the experimental results of this section we find evidence for an enhancement of the spin-splitting parameters ΔE and k_0 in the electronic structure of the surface alloy Bi/Cu(111) resulting from the adsorption of 0.1 ML monovalent Na atoms. In accordance with this the Rashba-parameter α increases by approximately 10%.

3.3. Xe-adsorption on Bi/Cu(111)

The modification of the electronic structure of Bi/Cu(111) by Xe-adsorption is first examined by considering the overview ARPES spectra in figure 6. Comparing the measurements before and after the adsorption we do not observe major changes in the dispersion of the surface states. A considerable shift to lower binding energies as was found for the surface state of Au(111) is not visible in the data. Instead the presence of the Xe-overlayer provokes the appearance of faint shadow bands which are marked by arrows in figure 6(b). A very similar situation was found in the case of Xe adsorbed on Bi/Ag(111) [33]. For this system the shadow bands were identified as backfolded replicas of the surface state branches based on a comparison to LEED measurements of the Xe-overlayer. Although at present no structural data for Xe/Bi/Cu(111) is available it seems plausible to assume the same origin of the shadow bands for both surface alloys. Another effect that is visible in the data in figure 6 is a change of the relative spectral weight of the individual branches. Especially, the intensity of the band E_- at negative wave vectors is strongly reduced after the adsorption. This effect could be caused by scattering effects of the photoelectrons that are induced by the Xe-overlayer.

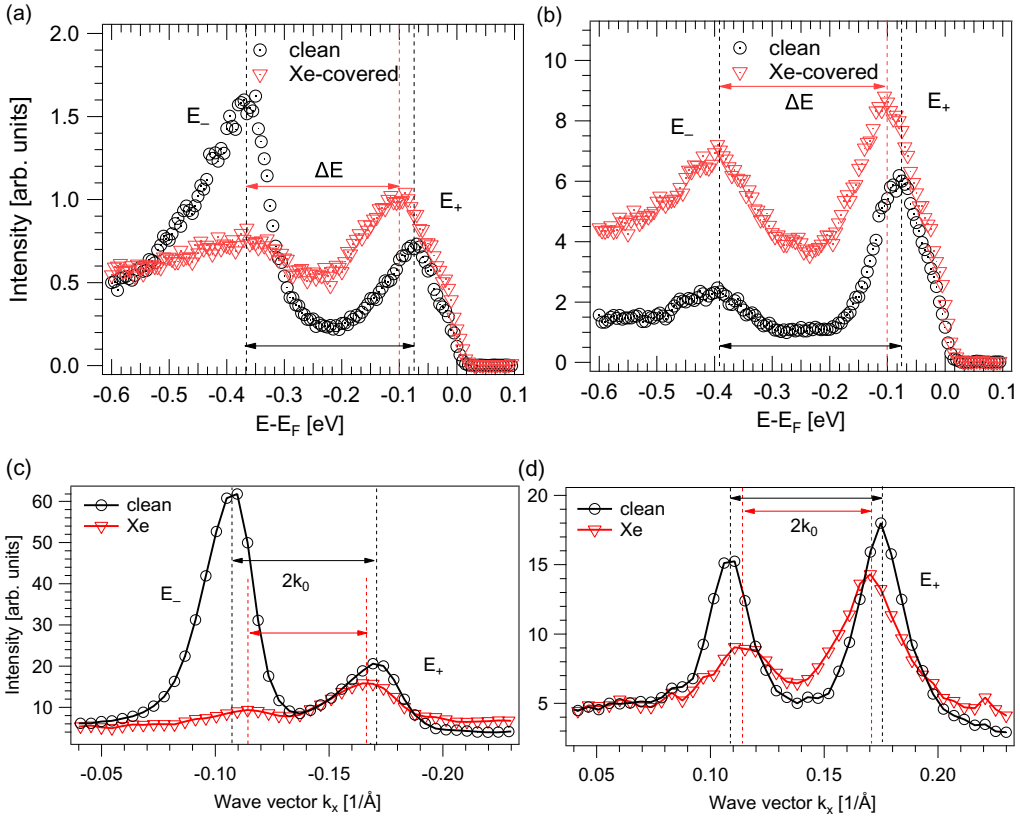

Figure 7. EDC at $k_x = -0.19$ and $0.2\ \text{Å}^{-1}$ in (a) and (b) and MDC at the Fermi energy E_F in (c) and (d) for Bi/Cu(111) before and after deposition of $\sim$1 ML Xe. All EDC and MDC show two peaks that are associated with the spin-split branches E_+ and E_-. The corresponding energy separations ΔE and wave vector offsets k_0 are indicated.

To investigate the influence of Xe-adsorption on the spin-splitting parameter ΔE we consider EDC in figure 7 corresponding to the ARPES spectra in figure 6. Panels (a) and (b) show EDC at $k_x = -0.19$ and $+0.2\ \text{Å}^{-1}$ for clean and Xe-covered Bi/Cu(111). In each EDC one can identify two peaks being associated with the two branches E_+ and E_-. As is evident from the data the separation between these peaks and thus the energy splitting ΔE is reduced as a result of the adsorption.

A similar result is obtained by investigating the wave vector offset k_0 by means of MDC at E_F in figures 7(c) and (d). As is evident from the spectra the peaks corresponding to the branches E_+ and E_- are shifted slightly toward each other as a result of Xe-adsorption. Hence, the wave vector splitting k_0 is reduced.

In figure 8 we present an analysis of the dispersion of the state $E_\pm$ based on MDC. The left four panels show detail plots for clean and Xe-covered Bi/Cu(111). The data points in these graphs denote intensity maxima. The corresponding wave vector offsets k_0 are plotted as a function of energy in figure 8(e). The energy axes in figure 8 are divided into the two intervals I and II according to the discussion of the clean surface alloy in section 3.2. One recognizes small deviations between the values for k_0 along positive and negative wave vectors occurring

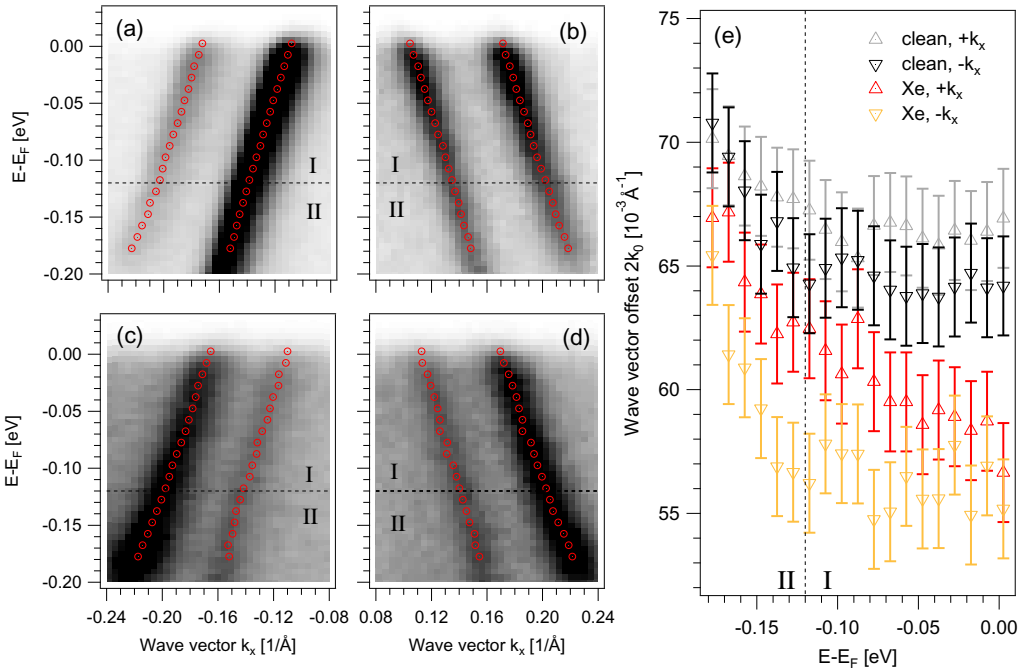

Figure 8. Quantitative analysis of the Rashba-split branches $E_{\pm}$ in Bi/Cu(111) before and after adsorption of ∼1 ML Xe. Detail plots for the clean and the Xe-covered surface alloy are shown in (a), (b) and (c), (d), respectively. The data points in these panels denote intensity maxima. The corresponding wave vector offsets k_0 are plotted in (e).

both for the clean and the Xe-covered surface alloy. We reckon these discrepancies to originate from a slight misalignment of the sample during the measurement. Comparing the determined wave vector offsets one finds a significant reduction of k_0 within interval I resulting from the adsorption. In interval II the situation is less clear and the reduction appears to decrease and eventually vanish. A least-square fit of equation (1) to the data points in figure 8 within interval I yields Rashba-parameters of $\alpha = 0.83(3)$ eV Å for clean Bi/Cu(111) and $\alpha = 0.73(3)$ eV Å for Xe-covered Bi/Cu(111).

Summarizing this section the measurements indicate a reduction of the spin-splitting parameters ΔE and k_0 in the electronic structure of Bi/Cu(111) as a result of the adsorption of ∼1 ML closed-shell Xe. Accordingly the Rashba-parameter α decreases approximately by 10%.

4. Discussion

The main results of the previous sections are an enhancement and a reduction of the Rashba-splitting in the surface alloy Bi/Cu(111) that are induced by the adsorption of monovalent Na and closed-shell Xe, respectively. In the most basic approximation the size of the spin-splitting is expected to scale with the atomic numbers Z of the contributing elements. This approach, however, can explain neither a larger splitting for the Na-covered ($Z = 11$) than for the Xe-covered ($Z = 54$) surface alloy nor an increased splitting of a Bi-derived ($Z = 83$) state after

Na-adsorption. In order to discuss the experimental results we will thus adopt a more elaborate model for the Rashba-parameter α leading to the following expression [16]:

$$\alpha = 2/c^2 \int \phi^2(z)\partial_z V \mathrm{d}^3\boldsymbol{r}. \tag{2}$$

Here, $\phi^2(z)$ is the partial charge distribution of the surface state along the surface normal z. Theoretical works based on density functional theory showed that the integral in equation (2) is determined basically in a very small region around the atomic core where the potential gradient $\partial_z V$ becomes largest and follows a Coulomb-behavior [15, 16]. However, also the surface potential is of critical importance as it determines the precise form of $\phi^2(z)$. Note that according to equation (2) α is essentially determined by the imbalance of $\phi^2(z)$ around the core because on has $\partial_z V(-z) \approx -\partial_z V(z)$. Considering equation (2) adsorbate-induced changes of α are simply understood as a modification of $\phi^2(z)$ whereas $\partial_z V$ remains unchanged.

The influence of alkali and rare gas adsorption on metallic surface states is extensively discussed in the literature (see e.g. [30, 44–46]). Alkali atoms induce a reduction of the work function and are thus expected to lower the surface potential barrier. The interaction of rare gases with substrate states, on the other hand, is often dominated by the Pauli-repulsion resulting from the overlap of filled valence orbitals of the rare gas atoms and substrate wave functions leaking into the vacuum [47]. The Pauli-repulsion gives rise to an effective increase of the surface potential. The opposite effects of the two adsorbate species on the Rashba-splitting thus appear reasonable and may result from opposite influences on the surface state wave function.

A comparison to experimental results for Xe/Au(111), however, reveals the necessity for a more detailed analysis. In this system α is increased by the adsorption [29], in contrast to the present findings for Bi/Cu(111). It has been shown previously that the surface state wave functions in these two systems show major differences. In the case of Bi/Cu(111) the surface state forms a bond between the Bi-atoms and the substrate. It is therefore predominantly localized between the two, that is on the substrate side of the Bi-cores [39]. For Au(111), however, the Shockley-type surface state is mostly localized between the topmost layer and the vacuum, that is on the vacuum side of the Au-cores [16, 48]. Thus, according to equation (2), the wave functions predominantly pick up a positive potential gradient in the case of Au(111) and a negative one in the case of Bi/Cu(111).

Let us examine the implications of these different wave functions by considering the simple, purely schematic sketch in figure 9. As has been argued before the increase of the Rashba-splitting in Au(111) after Xe-adsorption can be attributed to the Pauli-repulsion that pushes the surface state wave function closer to the nucleus [29]. This situation is sketched in figure 9(a) where we also make the simplifying assumption of a negligible influence of the adsorbate on the substrate-facing side of the charge distribution. Indeed equation (2) predicts an increase of α for this case as the already dominating contribution at positive potential gradients is further enhanced. In figure 9(b) we consider an analogue situation for Xe on Bi/Cu(111). If we again assume the surface-facing part of the charge distribution to move toward the atomic core the Rashba-parameter, or more precisely its absolute value, will decrease. This is due to the fact that for Bi/Cu(111) the contribution at negative gradients is dominating and an increased contribution at positive gradients will therefore lead to a reduction of α. As discussed above Na atoms lower the surface potential barrier which can be viewed as the introduction of an effective attractive potential. In this case one can expect the surface-facing part of the charge distribution to move away from the core toward the vacuum as depicted

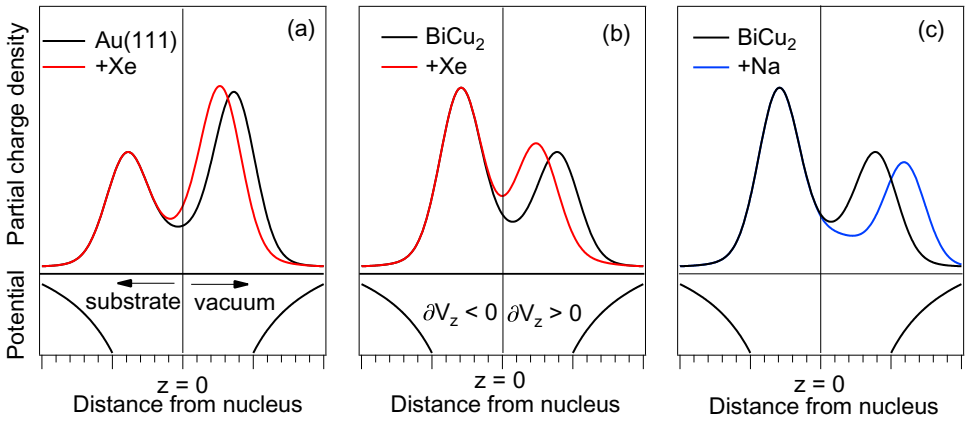

Figure 9. Schematic illustration of the surface state charge distribution and its modification by adsorbates for Au(111) in (a) and for Bi/Cu(111) in (b) and (c). Only one atomic layer at $z = 0$ is considered, representing the topmost surface layer in the case of Au(111) and the Bi-layer in the case of Bi/Cu(111). The charge distributions for the clean surfaces are predominantly localized on the vacuum-facing side of the atomic cores ($\partial_z V > 0$) for Au(111) and on the substrate-facing side ($\partial_z V < 0$) for Bi/Cu(111). The adsorption of Xe induces a shift of the vacuum-facing part of the charge distribution toward the atomic core, whereas the adsorption of Na gives rise to the opposite effect (see text for details). The influence of the depicted charge distribution changes on the Rashba-parameter as predicted by equation (2) is in qualitative agreement with the experimentally observed trends.

schematically in figure 9(c). For this situation equation (2) predicts an increase of the Rashba-parameter because the already weaker contribution at positive potential gradients is further reduced. Hence, by making plausible assumptions for modifications of the surface state charge distributions the experimentally observed changes of the Rashba-parameter α can be reconciled using equation (2). Thus, both the character of the surface state wave function and the chemical properties of the adsorbate play a decisive role in determining the change of α. It would be desirable to compare the simple model in figure 9 with *ab initio* calculations in order to gain a more realistic view on the electronic charge distribution [49].

Despite the agreement between the experimental findings and the model considerations certain unclarities are remaining. The validity of the assumption of a repulsive potential change in the case of Xe/Bi/Cu(111) is not clear. In a simple picture a repulsive potential is associated with a reduced binding energy which is experimentally found for Xe/Au(111) but not for Xe/Bi/Cu(111). Furthermore, we have not considered possible structural changes as a result of the adsorption which may give rise to additional modifications of α being not directly related to the chemical nature of the adsorbate [50].

It is instructive to compare the present results to previous studies on the Rashba effect in related systems. For the adsorption of Xe on the surface alloy Bi/Ag(111) no change of the Rashba-parameter was found [33]. The splitting in Bi/Ag(111) is four times larger than in Bi/Cu(111) [25] and therefore, according to equation (2), the surface state charge distribution should show an even higher weight on the substrate side of the Bi atoms. This could result

in a reduced sensitivity to adatoms. Another possibility is the important role of in-plane potential gradients in Bi/Ag(111) [20, 51] that might be expected to be rather insensitive to adsorbates [33]. For the case of W(110) alkali adsorption induces an enhanced splitting similar to the present findings for Bi/Cu(111) [28].

5. Conclusions

Based on ARPES experiments we have shown that the Rashba-splitting in the surface alloy Bi/Cu(111) can be enhanced and reduced by adsorption of monovalent Na and closed-shell Xe, respectively. The opposite changes in the splitting size are likely due to the different chemical nature of the two adsorbate species and thus different influences on the states in the surface alloy. Our study thus provides an example for a systematic modification of the Rashba-splitting by suitable changes of the surface chemical environment. It would be interesting to explore the applicability of this procedure for other adsorbate–substrate combinations. Comparing our results to Xe/Au(111) shows that a particular adsorbate may lead to opposite changes in the Rashba-splitting depending on the particular substrate. This is attributed to the different wave function character in the systems Au(111) and Bi/Cu(111). A proper understanding of adsorbate-induced modifications of the Rashba-splitting requires detailed knowledge about the microscopic charge distribution of the surface states. Hence, *ab initio* calculations, based e.g. on density functional theory, that explicitly take these microscopic aspects into account are inevitable to acquire a predictive power for the Rashba effect at surfaces. In agreement with previous works our results indicate the asymmetry of the charge distribution close to the atomic cores to be an important parameter for the size of the Rashba-splitting.

Acknowledgments

We would like to thank Frank Forster and Gustav Bihlmayer for valuable discussions. HB acknowledges experimental support by Andreas Nuber and Johannes Ziroff. This work was supported by the Bundesministerium für Bildung und Forschung (grant numbers 05K10WW1/2 and 05KS1WMB/1) and the Deutsche Forschunsgsgemeinschaft within the Forschergruppe 1162.

References

[1] Winkler R 2003 *Spin–Orbit Coupling Effects in Two-Dimensional Electron and Hole Systems* (*Springer Tracts in Modern Physics* vol 191) ed G Höhler, J Kühn, Th Müller, A Ruckenstein, F Steiner, J Trümper and P Wölfle (Berlin: Springer) pp 69–129

[2] Bychkov Yu A and Rashba E I 1984 Properties of a 2D electron-gas with lifted spectral degeneracy *JETP Lett.* **39** 78

[3] Datta S and Das B 1990 Electronic analog of the electro-optic modulator *Appl. Phys. Lett.* **56** 665

[4] Nitta J, Akazaki T, Takayanagi H and Enoki T 1997 Gate control of spin–orbit interaction in an inverted $In_{0.53}Ga_{0.47}As/In_{0.52}Al_{0.48}As$ heterostructure *Phys. Rev. Lett.* **78** 1335–8

[5] Koo H C, Kwon J H, Eom J, Chang J, Han S H and Johnson M 2009 Control of spin precession in a spin-injected field effect transistor *Science* **325** 1515–8

[6] Sinova J, Culcer D, Niu Q, Sinitsyn N A, Jungwirth T and MacDonald A H 2004 Universal intrinsic spin Hall effect *Phys. Rev. Lett.* **92** 126603

[7] Potter A C and Lee P A 2010 Multichannel generalization of Kitaev's Majorana end states and a practical route to realize them in thin films *Phys. Rev. Lett.* **105** 227003
[8] Potter A C and Lee P A 2012 Topological superconductivity and Majorana fermions in metallic surface states *Phys. Rev.* B **85** 094516
[9] Mourik V, Zuo K, Frolov S M, Plissard S R, Bakkers E P A M and Kouwenhoven L P 2012 Signatures of Majorana fermions in hybrid superconductor–semiconductor nanowire devices *Science* **336** 1003–7
[10] Zarea M, Ulloa S E and Sandler N 2012 Enhancement of the Kondo effect through Rashba spin–orbit interactions *Phys. Rev. Lett.* **108** 046601
[11] Cappelluti E, Grimaldi C and Marsiglio F 2007 Topological change of the Fermi surface in low-density Rashba gases: application to superconductivity *Phys. Rev. Lett.* **98** 167002
[12] Caviglia A D, Gabay M, Gariglio S, Reyren N, Cancellieri C and Triscone J-M 2010 Tunable Rashba spin–orbit interaction at oxide interfaces *Phys. Rev. Lett.* **104** 126803
[13] Petersen L and Hedegård P 2000 A simple tight-binding model of spin–orbit splitting of sp-derived surface states *Surf. Sci.* **459** 49
[14] Majewski J A and Vogl P 2003 Resonant spin–orbit interactions and phonon relaxation rates in superlattices *Physics of Semiconductors 2002* ed A R Long and J H Davies (Bristol: IOP) p 305
[15] Bihlmayer G, Koroteev Yu M, Echenique P M, Chulkov E V and Blügel S 2006 The Rashba-effect at metallic surfaces *Surf. Sci.* **600** 3888–91
[16] Nagano M, Kodama A, Shishidou T and Oguchi T 2009 A first-principles study on the Rashba effect in surface systems *J. Phys.: Condens. Matter* **21** 064239
[17] Vajna Sz, Simon E, Szilva A, Palotas K, Ujfalussy B and Szunyogh L 2012 Higher-order contributions to the Rashba–Bychkov effect with application to the Bi/Ag(111) surface alloy *Phys. Rev.* B **85** 075404
[18] LaShell S, McDougall B A and Jensen E 1996 Spin splitting of an Au(111) surface state band observed with angle resolved photoelectron spectroscopy *Phys. Rev. Lett.* **77** 3419–22
[19] Koroteev Yu M, Bihlmayer G, Gayone J E, Chulkov E V, Blügel S, Echenique P M and Hofmann P 2004 Strong spin–orbit splitting on Bi surfaces *Phys. Rev. Lett.* **93** 046403
[20] Ast C R, Henk J, Ernst A, Moreschini L, Falub M C, Pacilé D, Bruno P, Kern K and Grioni M 2007 Giant spin splitting through surface alloying *Phys. Rev. Lett.* **98** 186807
[21] Hüfner S 1994 *Photoelectron Spectroscopy* (Berlin: Springer)
[22] Popović D, Reinert F, Hüfner S, Grigoryan V G, Springborg M, Cercellier H, Fagot-Revurat Y, Kierren B and Malterre D 2005 High-resolution photoemission on Ag/Au(111): spin–orbit splitting and electronic localization of the surface state *Phys. Rev.* B **72** 045419
[23] Cercellier H, Didiot C, Fagot-Revurat Y, Kierren B, Moreau L, Malterre D and Reinert F 2006 Interplay between structural, chemical and spectroscopic properties of Ag/Au(111) epitaxial ultrathin films: a way to tune the Rashba coupling *Phys. Rev.* B **73** 195413
[24] Shikin A M, Varykhalov A, Prudnikova G V, Usachov D, Adamchuk V K, Yamada Y, Riley J D and Rader O 2008 Origin of spin–orbit splitting for monolayers of Au and Ag on W(110) and Mo(110) *Phys. Rev. Lett.* **100** 057601
[25] Bentmann H, Forster F, Bihlmayer G, Chulkov E V, Moreschini L, Grioni M and Reinert F 2009 Origin and manipulation of the Rashba splitting in surface alloys *Europhys. Lett.* **87** 37003
[26] Gierz I, Stadtmüller B, Vuorinen J, Lindroos M, Meier F, Dil J H, Kern K and Ast C R 2010 Structural influence on the Rashba-type spin splitting in surface alloys *Phys. Rev.* B **81** 245430
[27] Slomski B, Landolt G, Meier F, Patthey L, Bihlmayer G, Osterwalder J and Dil J H 2011 Manipulating the Rashba-type spin splitting and spin texture of Pb quantum well states *Phys. Rev.* B **84** 193406
[28] Rotenberg E, Chung J W and Kevan S D 1999 Spin–orbit coupling induced surface band splitting in Li/W(110) and Li/Mo(110) *Phys. Rev. Lett.* **82** 4066–9
[29] Reinert F 2003 Spin–orbit interaction in the photoemission spectra of noble metal surface states *J. Phys.: Condens. Matter* **15** S693–705
[30] Forster F, Bendounan A, Ziroff J and Reinert F 2006 Systematic studies on surface modifications by ARUPS on Shockley-type surface states *Surf. Sci.* **600** 3870–4

[31] Forster F, Bendounan A, Reinert F, Grigoryan V G and Springborg M 2007 The Shockley-type surface state on Ar covered Au(111): high resolution photoemission results and the description by slab-layer DFT calculations *Surf. Sci.* **601** 5595–604
[32] Krupin O, Bihlmayer G, Starke K, Gorovikov S, Prieto J E, Döbrich K, Blügel S and Kaindl G 2005 Rashba effect at magnetic metal surfaces *Phys. Rev.* B **71** 201403
[33] Moreschini L, Bendounan A, Ast C R, Reinert F, Falub M and Grioni M 2008 Effect of rare-gas adsorption on the spin–orbit split bands of a surface alloy: Xe on Ag(111)-$(\sqrt{3}\times\sqrt{3})R30^{\circ}$−Bi *Phys. Rev.* B **77** 115407
[34] Meier F, Dil H, Lobo-Checa J, Patthey L and Osterwalder J 2008 Quantitative vectorial spin analysis in angle-resolved photoemission: Bi/Ag(111) and Pb/Ag(111) *Phys. Rev.* B **77** 165431
[35] Moreschini L, Bendounan A, Bentmann H, Assig M, Kern K, Reinert F, Henk J, Ast C R and Grioni M 2009 Influence of the substrate on the spin–orbit splitting in surface alloys on (111) noble-metal surfaces *Phys. Rev.* B **80** 035438
[36] Akin Ünal A, Winkelmann A, Tusche C, Bisio F, Ellguth M, Chiang C-T, Henk J and Kirschner J 2012 Polarization dependence and surface sensitivity of linear and nonlinear photoemission from Bi/Cu(111) *Phys. Rev.* B **86** 125447
[37] Steinbrecher M, Harutyunyan H, Ast C R and Wegner D 2013 Rashba-type spin splitting from interband scattering in quasiparticle interference maps *Phys. Rev.* B **87** 245436
[38] Mirhosseini H, Henk J, Ernst A, Ostanin S, Chiang C-T, Yu P, Winkelmann A and Kirschner J 2009 Unconventional spin topology in surface alloys with Rashba-type spin splitting *Phys. Rev.* B **79** 245428
[39] Bentmann H, Kuzumaki T, Bihlmayer G, Blügel S, Chulkov E V, Friedrich Reinert and Kazuyuki Sakamoto 2011 Spin orientation and sign of the Rashba splitting in Bi/Cu(111) *Phys. Rev.* B **84** 115426
[40] Pacilé D, Ast C R, Papagno M, Da Silva C, Moreschini L, Falub M C, Seitsonen P A and Grioni M 2006 Electronic structure of an ordered Pb/Ag(111) surface alloy: theory and experiment *Phys. Rev.* B **73** 245429
[41] Henk J, Scheunemann T, Halilov S V and Feder R 1996 Magnetic dichroism and electron spin polarization in photoemission: analytical results *J. Phys.: Condens. Matter* **8** 47–65
[42] Bentmann H, Abdelouahed S, Mulazzi M, Henk J and Reinert F 2012 Direct observation of interband spin–orbit coupling in a two-dimensional electron system *Phys. Rev. Lett.* **108** 196801
[43] Crepaldi A, Pons S, Frantzeskakis E, Kern K and Grioni M 2012 Anisotropic spin gaps in $BiAg_2$-Ag/Si(111) *Phys. Rev.* B **85** 075411
[44] Lindgren S Å and Walldén L 1978 Cu surface state and Cs valence electrons in photoelectron spectra from the Cu(111)/Cs adsorption system *Solid State Commun.* **28** 283–6
[45] Andreev T, Barke I and Hövel H 2004 Adsorbed rare-gas layers on Au(111): shift of the Shockley surface state studied with ultraviolet photoelectron spectroscopy and scanning tunneling spectroscopy *Phys. Rev.* B **70** 205426
[46] Bentmann H, Buchter A and Reinert F 2012 Interplay of electronic structure and atomic ordering on surfaces: momentum-resolved measurements of Cs atoms adsorbed on a Ag(111) substrate *Phys. Rev.* B **85** 121412
[47] Bertel E and Memmel N 1996 Promotors, poisons and surfactants: electronic effects of surface doping on metals *Appl. Phys.* A **63** 523–31
[48] Henk J, Hoesch M, Osterwalder J, Ernst A and Bruno P 2004 Spin–orbit coupling in the L-gap surface states of Au(111): spin-resolved photoemission experiments and first-principles calculations *J. Phys.: Condens. Matter* **16** 7581–97
[49] Lee H and Choi H J 2012 Role of *d* orbitals in the Rashba-type spin splitting for noble-metal surfaces *Phys. Rev.* B **86** 045437
[50] Bihlmayer G, Blügel S and Chulkov E V 2007 Enhanced Rashba spin–orbit splitting in Bi/Ag(111) and Pb/Ag(111) surface alloys from first principles *Phys. Rev.* B **75** 195414
[51] Premper J, Trautmann M, Henk J and Bruno P 2007 Spin–orbit splitting in an anisotropic two-dimensional electron gas *Phys. Rev.* B **76** 073310